Proceedings of the ASME 2022 41st International Conference on Ocean, Offshore and Arctic Engineering
OMAE2022
June 5-June 10, 2022, Hamburg, Germany

OMAE2022-78929

INFLUENCE OF AERODYNAMIC LOADS ON A DUAL-SPAR FLOATING OFFSHORE WIND FARM WITH A SHARED LINE IN PARKED CONDITIONS

Guodong Liang
Department of Engineering Sciences
University of Agder
N-4898 Grimstad, Norway

Zhiyu Jiang
Department of Engineering Sciences
University of Agder
N-4898 Grimstad, Norway

Karl Merz
SINTEF Energy Research
N-7034 Trondheim, Norway

ABSTRACT

The concept of a shared mooring system, in which adjacent wind turbines are coupled by sharing mooring lines, has been proposed to reduce the mooring costs of floating offshore wind farms. This work investigates the influence of aerodynamic loads on a floating offshore wind farm of two spar wind turbines connected with a shared line in extreme environmental conditions. A case study is performed for the floating offshore wind farm under parked conditions using a numerical simulation tool. The environmental conditions are determined from environmental contours with a return period of 50 years. Turbulent wind and irregular waves are simulated in dynamic analyses. Wind and waves are aligned and two loading directions are considered. Floater motions and structural response are analyzed. The influence of aerodynamic loads is studied by comparing the simulation results under both wind and waves with those under wave-only. It is concluded that the aerodynamic loads affect the horizontal motions of floating offshore wind turbines, the mooring response and the tower-base bending moment significantly in extreme environmental conditions, especially when the loading direction is 90 deg. The findings from this study improve understanding of the design loads of shared mooring systems.

1 INTRODUCTION

To chase the even stronger wind and with the consideration of less visual impact, a floating offshore wind farm (FOWF) becomes a promising engineering solution. Studies and research have been conducted to make floating offshore wind energy cost-competitive. A shared mooring system is one of the design innovations to reduce costs. By connecting adjacent floating offshore wind turbines (FOWTs) with a shared mooring line, the total number of mooring lines and the material costs are reduced. The number of anchors is reduced as well, which brings additional cost reduction. On the other hand, shared mooring lines integrate the whole FOWF as one floating system. The influence of coupling effects on system dynamic characteristics needs to be assessed thoroughly.

Gao and Moan [1] assessed the application of a shared mooring system on wave energy converters. Both time- and frequency-domain analyses were performed. Goldschmidt and Muskulus [2] studied dynamic properties and cost-saving potential of shared mooring systems for FOWTs. Simplified models were used and different configurations were investigated. A square-shaped FOWF with a shared mooring system was modeled and investigated by Hall and Connolly [3]. Complex restoring properties and a greater tendency of resonance caused by the shared mooring system were reported. In the following study by

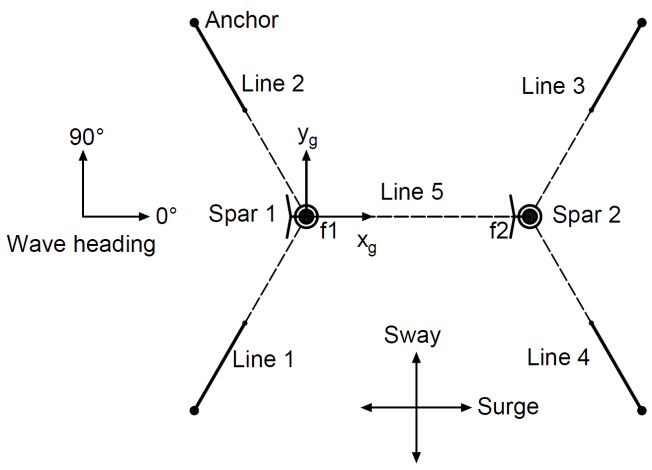

FIGURE 1: TOP VIEW OF THE DUAL-SPAR FOWF (DASHED LINE: WIRE, SOLID LINE: CHAIN)

Connolly and Hall [4], different configurations of shared mooring systems were compared for a square-shaped FOWF under varying water depths. In another work, Hall [5] studied the mooring failure scenario of a dual-semi-submersible FOWF with a shared line using time-domain simulations. Wilson et al. [6] presented a linearized method to model the force-horizontal displacement relationship of FOWTs with a shared mooring system. An optimization approach was proposed and different FOWF layouts were evaluated in the case study. Liang et al. [7] proposed a method to model the shared line by applying the theory in elastic catenary of cable structures. In another work, Liang et al. [8] extended the modeling method to a two-segment single line and investigated the influence of mooring properties of a shared mooring system on the natural periods and natural modes of a dual-spar FOWF.

To the authors' knowledge, the influence of aerodynamic loads on the extreme response of an FOWF with a shared mooring system has not been studied in detail. To address this specific issue, we investigate the influence of aerodynamic loads on a dual-spar FOWF with a shared mooring system in extreme environmental conditions. In the following, the dual-spar FOWF studied is described in Sec. 2. Numerical modeling of the FOWF is introduced in Sec. 3. Details of a case study are described in Sec. 4. The main results are analyzed and discussed in Sec. 5. Conclusions are made in Sec. 6

2 DUAL-SPAR FLOATING OFFSHORE WIND FARM

The dual-spar FOWF consists of two OC3 Hywind spar FOWTs [9, 10]. A top view of the configuration is sketched in Fig. 1. Two FOWTs, Spar 1 and Spar 2, are placed along the global surge direction, i.e., along the x_g-axis. The initial distance between two spars is 1000 m (approximately eight rotor diameters), a typical separation distance in large offshore wind farms. A shared line, Line 5, is used to connect two FOWTs. Each wind turbine is moored to the seabed through two single lines. All projected angles between mooring lines are 120 deg and all fairleads are located 70 m below the still water level (SWL). The single lines are two-segment and the shared line is one-segment. Mooring properties from a previous study [8] are used to model the mooring system and presented in Table 1. Because the delta connection of mooring lines is not modeled, additional yaw stiffness [10] is added to the system. Free decay tests are performed for the dual-spar FOWF model. Natural periods are estimated and summarized in Table 2, in which surge, sway, heave, roll, pitch and yaw are the six degrees of freedom (DOFs) of the rigid-body motions of FOWTs. The dual-spar FOWF has twelve natural periods and natural modes. For each DOF, natural mode 1 indicates that both FOWTs move or rotate in the same direction and natural mode 2 indicates that they move or rotate in opposite directions.

TABLE 1: PROPERTIES OF MOORING LINES

Mooring property	Single line lower segment	Single line upper segment	Shared line
Material	R3 studless chain	Steel wire rope	Steel wire rope
Length [m]	452.2	550	989.6
Diameter [mm]	115	90	90
Sheath thickness [mm]	-	10	10
Mass density [kg/m]	264.50	42.77	42.77
Weight in water [N/m]	2385.86	324.00	324.00
Extensional stiffness [N]	1.06E+09	7.64E+08	7.64E+08
Minimum breaking strength [N]	1.03E+07	8.38E+06	8.38E+06

TABLE 2: NATURAL PERIOD OF THE DUAL-SPAR FOWF

Eigenmode	Surge	Sway	Heave	Roll	Pitch	Yaw
Mode 1 [s]	135.51	76.25	31.13	29.48	29.47	8.36
Mode 2 [s]	63.52	75.64	31.03	29.48	29.46	8.34

3 NUMERICAL MODELING

Dynamic analyses of the dual-spar FOWF are performed in SIMA, a numerical simulation tool for marine operations [11, 12]. The wind turbines and spar floaters are modeled in SIMA according to [9, 10]. Viscous drag is modeled for the un-

derwater part of each spar floater. Mooring lines are modeled as slender structures in the RIFLEX module of SIMA. Slender structures are modeled by defining two endpoints as supernodes and specifying cross-section properties for different segments. Each segment consists of finite elements with the same cross-section properties. One hundred bar elements are used to model the single lines and the shared line. Fairleads and anchor points are modeled as supernodes. The FOWTs are initially placed such that the mooring lines are unloaded. After reaching the static equilibrium, the two turbines approach each other along the x_g-axis by a short distance, due to the self weight of the shared line.

A hydrodynamic analysis is performed for a single spar FOWT in WADAM, a linear potential-flow program [13]. Because the turbine spacing is large, the hydrodynamic coupling between the two spar FOWTs is ignored. The obtained hydrodynamic properties of the single FOWT, like the frequency-dependent hydrodynamic added mass and radiation damping coefficients, the first-order wave force transfer functions and the wave drift force, are imported into the dual-spar model in SIMA.

In the dynamic analyses, the FOWTs are parked (standing still) and the blades are feathered. Turbulent wind and irregular waves are simulated. Irregular waves are generated with random wave seeds. Wave forces are integrated to the mean water level. Turbulent wind fields are generated in Turbsim [14] and imported to SIMA. The size parameters of the wind field grid are determined with consideration of the tower structure and the heave motion of FOWTs, so that the FOWTs are always inside the turbulent wind field. For the parked rotors, steady lift and drag coefficients are used to calculate the aerodynamic loads. The airfoil coefficients of wind turbine blades specified in [9] are used. The drag force acting on the tower is modeled in SIMA by specifying drag coefficients. According to the offshore standard [15], aerodynamic drag force coefficients are set to 0.65 based on the Reynolds number calculation.

4 CASE STUDY

A case study is conducted to investigate the influence of aerodynamic loads on the extreme response of the dual-spar FOWF described in Sec. 2.

4.1 Metocean Conditions

A return period of 50 years is considered for the extreme loading conditions according to the offshore standard [16]. The water depth is 320 m as specified in the OC3 report [10]. The joint distribution of environmental condition of a European offshore site, 'Norway 5' [17], is used to determine the mean wind speed (U_w), the significant wave height (H_s) and the spectral peak period (T_p). The 50-year environmental contour surface is generated from the joint distribution and the sea state on the contour surface with the highest H_s is selected. According to the design standards [18, 19], the wind turbine class I-B is chosen, and the IEC Normal Turbulence Model is used.

TABLE 3: ENVIRONMENTAL PARAMETERS FOR THE DYNAMIC ANALYSIS

Environmental parameter	Value
U_w (Hub-height) [m/s]	42.71
I (Turbulence intensity) [-]	0.12
H_s [m]	15.50
T_p [s]	14.45
Loading direction [deg]	0, 90

To investigate the influence of aerodynamic loads, both combined wind and wave conditions and wave-only conditions are simulated. For wave-only conditions, only irregular waves are simulated. For combined wind and wave conditions, turbulent wind and irregular waves are simulated in the same direction. Two different loading directions, 0 deg and 90 deg (see Fig. 1), are considered. The environmental parameters are listed in Table 3.

4.2 Dynamic Analysis

A convergence study is conducted to determine the number of realizations for simulations in each environmental condition. Both floater motions and structural responses are checked. From the results, it is concluded that twenty 1-hour realizations are sufficient for the extreme response statistics to reach convergence. Therefore, for each loading condition, twenty 1-hour time-domain simulations are performed in SIMA for the dual-spar FOWF model. The results of floater motions and structural responses are read into MATLAB for further analysis.

5 RESULTS AND DISCUSSION

The results are analyzed and presented in the following sections. In the figures, 'Wind and wave' refers to results from dynamic analyses under combined wind and wave conditions and 'Wave-only' refers to those under wave-only conditions.

5.1 Spar-platform Motions

Considering the station-keeping purpose of the mooring system and the integrity of the power cable, the horizontal offset of FOWTs needs to be limited. Therefore, the horizontal motions of FOWTs are of interest.

Time series of the body origins of FOWTs are obtained from dynamic simulations. For each 1-hour realization, the mean dy-

TABLE 4: POSITIONS OF BODY ORIGINS IN DIFFERENT CONDITIONS

Condition	Spar 1		Spar 2	
	x [m]	y [m]	x [m]	y [m]
Initial position	0	0	1000	0
Static position	2.56	0	997.70	0
Mean dynamic position (0 deg, wave-only)	3.99	0.02	996.35	-0.01
Mean dynamic position (0 deg, wind and wave)	13.59	0.35	1006.25	3.71
Mean dynamic position (90 deg, wave-only)	3.54	0.11	997.17	0.12
Mean dynamic position (90 deg, wind and wave)	1.95	11.36	996.79	11.09

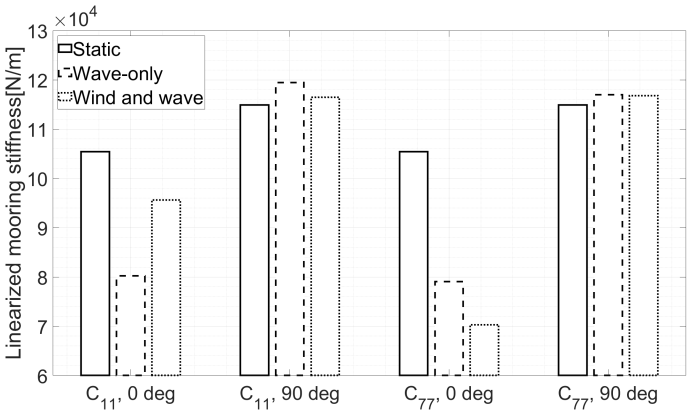

FIGURE 2: LINEARIZED MOORING STIFFNESS TERMS

namic positions of body origins are computed. Positions of body origins in the initial configuration, in the static condition and the mean value over twenty realizations, are presented in Table 4. As discussed in Sec. 3, the offsets of static positions from the initial positions are due to the self weight of the shared line. Compared with static positions, small offsets of mean positions under wave-only conditions are observed. Large offsets along the loading direction are observed in the mean positions of body origins under combined wind and wave conditions. With the mean positions under wave-only conditions as the reference, it is clear that the aerodynamic loads acting on the FOWTs lead to these large offsets. As a result, the mooring stiffness of the floating system varies significantly from the wave-only conditions to the combined wind and wave conditions.

The method to calculate the linearized mooring stiffness of a shared mooring system presented in [8] is applied to compute the linearized mooring stiffness of the dual-spar FOWF. Only the rigid-body motions of FOWTs in six DOFs are considered, namely surge, sway, heave, roll, pitch and yaw. Hence the linearized mooring stiffness matrix of the FOWF is a 12×12 matrix.

TABLE 5: MEAN MOTION RANGE OF BODY ORIGINS ALONG THE LOADING DIRECTION IN DIFFERENT LOADING CONDITIONS

Loading direction	Spar 1		Spar 2	
	Wave-only [m]	Wind and wave [m]	Wave-only [m]	Wind and wave [m]
0 deg	[-11.12, 11.41]	[-12.40, 12.90]	[-11.54, 11.37]	[-12.76, 12.95]
90 deg	[-10.99, 11.22]	[-12.72, 13.61]	[-10.98, 11.22]	[-12.94, 13.16]

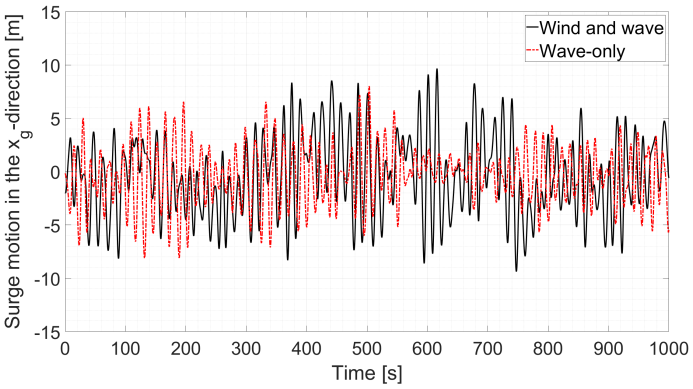

(a) Loading direction = 0 deg

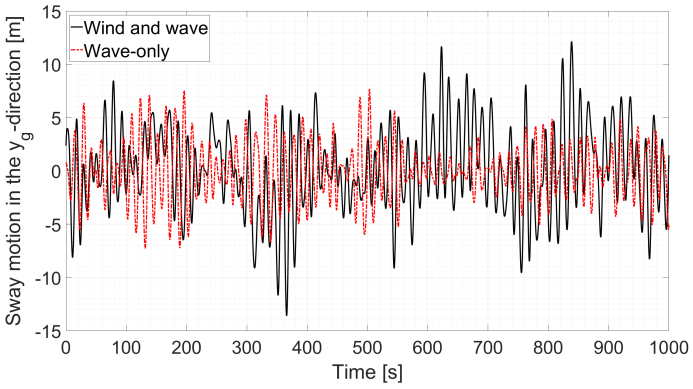

(b) Loading direction = 90 deg

FIGURE 3: TIME SERIES OF BODY ORIGIN OSCILLATION IN THE LOADING DIRECTION WITH RESPECT TO THE MEAN POSITIONS, SPAR 1

The mooring stiffness is linearized in the loading direction, therefore the stiffness terms, C_{M11} and C_{M77}, are always related to the motion of FOWTs in the loading direction. Both the static positions and the mean dynamic positions are used as the equilibrium positions in linearization. From [8], it is known that the diagonal stiffness terms C_{11} and C_{77} only have contributions from mooring stiffness. The stiffness terms of the FOWF, C_{11} and C_{77}, are plotted in Fig. 2. Due to different mean dynamic positions, a dif-

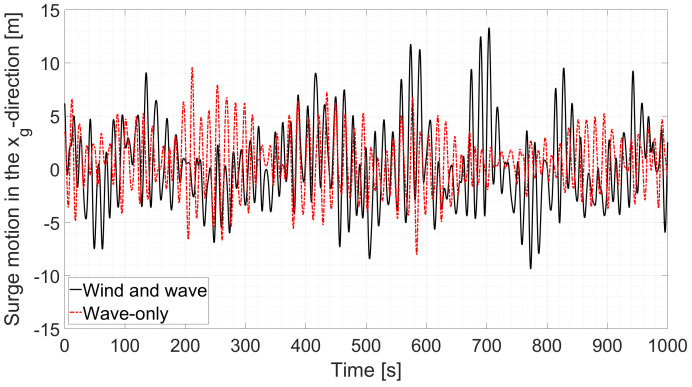

(a) Loading direction = 0 deg

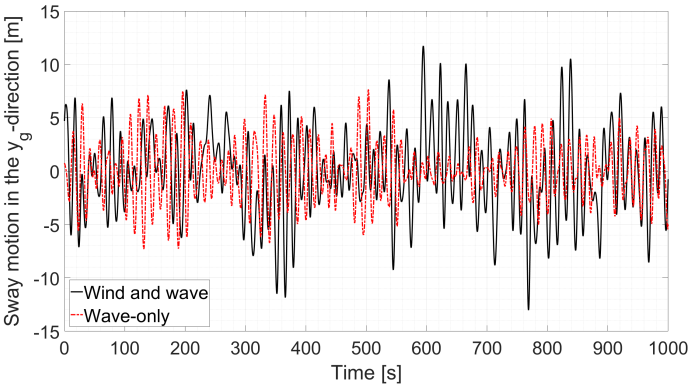

(b) Loading direction = 90 deg

FIGURE 4: TIME SERIES OF BODY ORIGIN OSCILLATION IN THE LOADING DIRECTION WITH RESPECT TO THE MEAN POSITIONS, SPAR 2

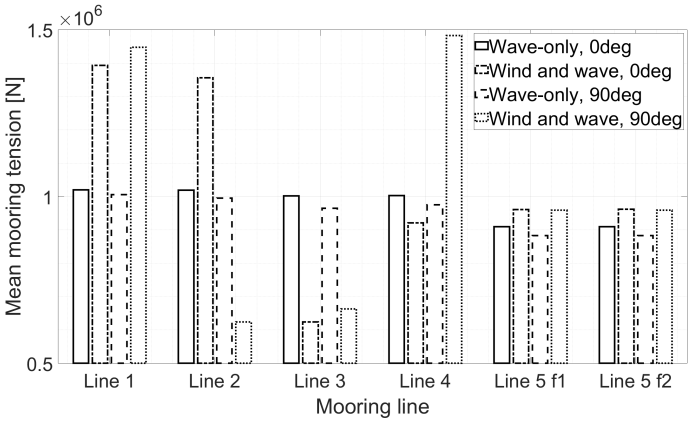

(a) Mean value

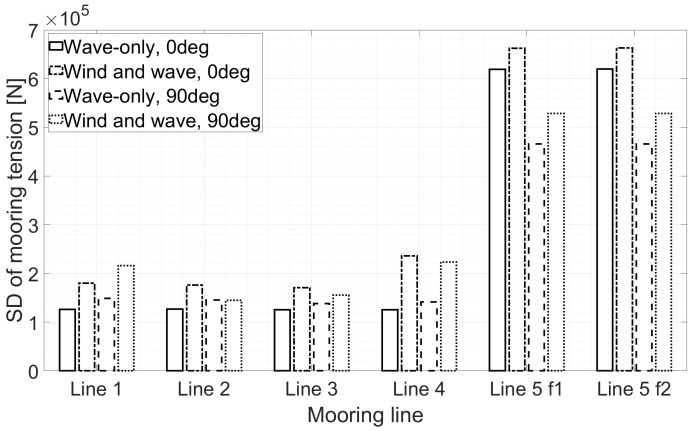

(b) SD

FIGURE 5: STATISTICS OF MOORING TENSION

ference of both C_{11} and C_{77} is observed between the wave-only conditions and the combined wind and wave conditions, especially when loading direction is 0 deg and the shared line plays an important role in the system mooring stiffness.

Taking the mean dynamic positions as a reference, the horizontal motions of FOWTs are projected to the loading direction. The mean value of the motion ranges in the loading direction is computed over twenty realizations and the results are presented in Table 5. Due to the presence of aerodynamic loads, larger motion ranges in the loading direction are observed under combined wind and wave conditions compared with those under wave-only conditions, especially when the loading direction is 90 deg and higher aerodynamic loads acting on the FOWTs are observed. Time series of body origin motions in the loading direction is presented in Fig. 3 and Fig. 4. It is clearly shown that under combined wind and wave conditions, the oscillation ranges are larger compared with those under wave-only conditions.

5.2 Mooring Response

The mooring tension at fairleads is investigated. The statistics of mooring tension are calculated for each 1-hour realization under different loading conditions. The mean value of mooring tension statistics over twenty realizations is computed. The mean value is presented in Fig. 5(a) and the standard deviation (SD) is presented in Fig. 5(b). From Fig. 5(a), it is seen that the mean tension of the single lines is significantly influenced by different loading conditions, but the influence on the shared line is limited. This is due to the fact that for the single lines, the mean mooring tension is related to the mean position of the fairlead, which moves together with the body origins of FOWTs. The mean positions of body origins under combined wind and wave conditions have large offsets compared to those under wave-only conditions; so does the mean mooring tension in single lines. For the shared line, the relative position of two fairleads determines the mooring tension. For different loading conditions, the difference of mean distance between body origins is relatively small;

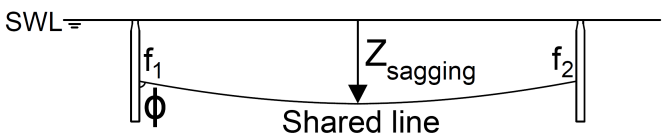

FIGURE 6: ILLUSTRATION OF MOORING ANGLE ϕ AND SAGGING DEPTH $Z_{sagging}$

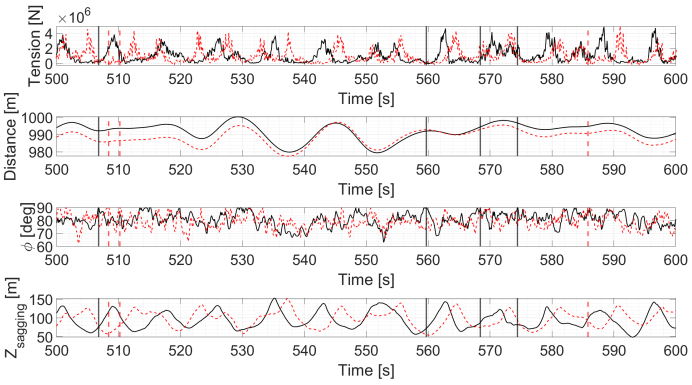

FIGURE 7: TIME SERIES OF THE TENSION AT THE FAIRLEAD LINE 5 F1, THE HORIZONTAL DISTANCE BETWEEN BODY ORIGINS, THE MOORING ANGLE AT THE FAIRLEAD LINE 5 F1, AND THE SAGGING DEPTH OF THE SHARED LINE (BLACK SOLID LINE: WIND AND WAVE, RED DASHED LINE: WAVE-ONLY)

so is the mean tension in the shared line.

Two parameters, the mooring angle and the sagging depth, are defined to investigate the profile of the shared line in dynamic simulations. As illustrated in Fig. 6, the mooring angle, ϕ, is defined as the angle between the mooring line and the vertical direction at the fairlead. The sagging depth, $Z_{sagging}$, is defined as the vertical distance from the lowest point on the shared line to the SWL (see Fig. 6). Time series of mooring responses of the shared line are plotted in Fig. 7 for the 0-deg loading conditions. In Fig. 7, time instants where ϕ is close to 90 deg are marked in all mooring responses. From Fig. 7, it is observed that there are correlations among the distance of body origins, the mooring angle and the value of $Z_{sagging}$. Maximum distance of the body origins means two FOWTs are most away from each other and the shared line is tightened. Therefore, the mooring angle is close to 90 deg and the value of $Z_{sagging}$ is reaching a minimum. The peaks of the mooring angle and tension do not occur simultaneously, and a time delay is observed between those.

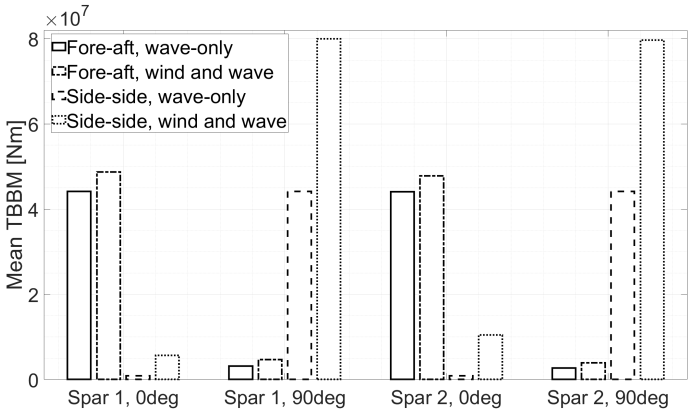

(a) Mean value

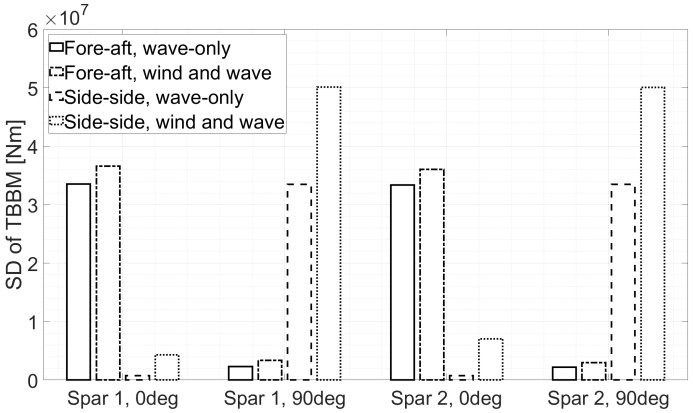

(b) SD

FIGURE 8: STATISTICS OF TBBM (ABSOLUTE VALUE)

5.3 Tower-base Bending Moment

The tower-base bending moments (TBBMs) are investigated. Statistics of the TBBMs (absolute value) are calculated for both FOWTs in each realization. The mean value over twenty realizations is computed. The mean value is presented in Fig. 8(a) and the SD is presented in Fig. 8(b). From Fig. 8, when the loading direction is 0 deg, the difference of the fore-aft TBBM statistics is not large between the results under the wave-only condition and those under the combined wind and wave condition. The difference between the side-side TBBM statistics is significant when the loading direction is 90 deg. This is because the blades of FOWTs are feathered in extreme environmental conditions. Due to the lift forces acting on the blades, the aerodynamic loads acting on the rotor are higher when the loading direction is 90 deg compared with the aerodynamic loads when the loading direction is 0 deg.

6 CONCLUSION

This paper presents an investigation of the influence of aerodynamic loads on the extreme response of a dual-spar floating offshore wind farm with a shared mooring system. A model of the dual-spar floating offshore wind farm has been established in the numerical simulation tool, SIMA. Dynamic analyses under different extreme conditions have been performed for the model in a case study. The motions of floating offshore wind turbines and different structural responses have been investigated. It has been revealed that aerodynamic loads have a significant influence on the extreme response of the floating offshore wind farm. Though the wind turbine blades are feathered, the extreme response is not entirely wave-dominant. Therefore, the aerodynamic loads cannot be ignored when the wind turbines are parked for the extreme response analysis.

In future, it would be interesting to investigate how the mooring properties of the shared mooring system can affect the extreme response of such a floating system.

ACKNOWLEDGMENT

The authors acknowledge the financial support from the Norwegian Ministry of Education and Research granted through the Department of Engineering Sciences, University of Agder.

REFERENCES

[1] Gao, Z., and Moan, T., 2009. "Mooring system analysis of multiple wave energy converters in a farm configuration". In Proceedings of the 8th European Wave and Tidal Energy Conference, Uppsala, Sweden, pp. 7–10.

[2] Goldschmidt, M., and Muskulus, M., 2015. "Coupled mooring systems for floating wind farms". *Energy Procedia,* ***80***, pp. 255–262.

[3] Hall, M., and Connolly, P., 2018. "Coupled dynamics modelling of a floating wind farm with shared mooring lines". In ASME 2018 37th International Conference on Ocean, Offshore and Arctic Engineering, Madrid, Spain, American Society of Mechanical Engineers Digital Collection.

[4] Connolly, P., and Hall, M., 2019. "Comparison of pilot-scale floating offshore wind farms with shared moorings". *Ocean Engineering,* ***171***, pp. 172–180.

[5] Hall, M., 2020. Moordyn v2: New capabilities in mooring system components and load cases. Tech. rep., National Renewable Energy Lab.(NREL), Golden, CO (United States).

[6] Wilson, S., Hall, M., Housner, S., and Sirnivas, S., 2021. "Linearized modeling and optimization of shared mooring systems". *Ocean Engineering,* ***241***, p. 110009.

[7] Liang, G., Merz, K., and Jiang, Z., 2020. "Modeling of a shared mooring system for a dual-spar configuration". In International Conference on Offshore Mechanics and Arctic Engineering, Vol. 9: Ocean Renewable Energy, American Society of Mechanical Engineers.

[8] Liang, G., Jiang, Z., and Merz, K., 2021. "Mooring analysis of a dual-spar floating wind farm with a shared line". *Journal of Offshore Mechanics and Arctic Engineering,* ***143***(6), p. 062003.

[9] Jonkman, J., Butterfield, S., Musial, W., and Scott, G., 2009. Definition of a 5-MW reference wind turbine for offshore system development. Tech. Rep. NREL/TP-500-38060, National Renewable Energy Lab.(NREL), Golden, CO (United States).

[10] Jonkman, J., 2010. Definition of the Floating System for Phase IV of OC3. Tech. Rep. NREL/TP-500-47535, National Renewable Energy Lab.(NREL), Golden, CO (United States).

[11] SINTEF Ocean, 2019. SIMO 4.16.0 User Guide. Trondheim, Norway.

[12] SINTEF Ocean, 2019. RIFLEX 4.16.0 User Guide. Trondheim, Norway.

[13] DNV GL, 2019. SESAM user manual, wave analysis by diffraction and morison theory. Høvik, Norway.

[14] Jonkman, B. J., and Buhl Jr, M. L., 2006. Turbsim user's guide. Tech. rep., National Renewable Energy Lab.(NREL), Golden, CO (United States).

[15] DNV, 2010. Recommended practice DNV-RP-C205, Environmental conditions and environmental loads. Høvik, Norway.

[16] DNV GL, 2018. Standard DNVGL-ST-0119, Floating wind turbine structures. Høvik, Norway.

[17] Li, L., Gao, Z., and Moan, T., 2015. "Joint distribution of environmental condition at five european offshore sites for design of combined wind and wave energy devices". *Journal of Offshore Mechanics and Arctic Engineering,* ***137***(3).

[18] IEC, 2005. International standard IEC 61400-1, Wind turbines—Part 1: Design requirements. Geneva, Switzerland.

[19] IEC, 2009. International standard IEC 61400-3, Wind turbines—Part 3: Design requirements for offshore wind turbines. Geneva, Switzerland.